



ORIGINAL ARTICLE

The PI3K/Akt/GSK-3 β /ROS/eIF2B pathway promotes breast cancer growth and metastasis via suppression of NK cell cytotoxicity and tumor cell susceptibility

Fengjiao Jin^{1*}, Zhaozhen Wu^{1*}, Xiao Hu¹, Jiahui Zhang¹, Zihe Gao¹, Xiao Han¹, Junfang Qin¹,
Chen Li², Yue Wang^{1,3}

¹School of Medicine, Nankai University, Tianjin 300071, China; ²Institute of Biomedical Engineering, Chinese Academy of Medical Sciences & Peking Union Medical College, Tianjin 300192, China; ³State Key Laboratory of Medicinal Chemical Biology, Nankai University, Tianjin 300071, China

ABSTRACT

Objective: To examine the effect of pSer9-GSK-3 β on breast cancer and to determine whether the underlying metabolic and immunological mechanism is associated with ROS/eIF2B and natural killer (NK) cells.

Methods: We employed TWS119 to inactivate GSK-3 β by phosphorylating Ser9 and explored its effect on breast cancer and NK cells. The expression of GSK-3 β , natural killer group 2 member D (NKG2D) ligands, eIF2B was quantified by PCR and Western blot. We measured intracellular reactive oxygen species (ROS) and mitochondrial ROS using DCFH-DA and MitoSOXTM probe, respectively, and conducted quantitative analysis of cellular respiration on 4T1 cells with mitochondrial respiratory chain complex I/III kits.

Results: Our investigation revealed that TWS119 downregulated NKG2D ligands (H60a and Rae1), suppressed the cytotoxicity of NK cells, and promoted the migration of 4T1 murine breast cancer cells. Nevertheless, LY290042, which attenuates p-GSK-3 β formation by inhibiting the PI3K/Akt pathway, reversed these effects. We also found that higher expression of pSer9-GSK-3 β induced higher levels of ROS, and observed that abnormality of mitochondrial respiratory chain complex I/III function induced the dysfunction of GSK-3 β -induced electron transport chain, naturally disturbing the ROS level. In addition, the expression of NOX3 and NOX4 was significantly up-regulated, which affected the generation of ROS and associated with the metastasis of breast cancer. Furthermore, we found that the expression of pSer535-eIF2B promoted the expression of NKG2D ligands (Mult-1 and Rae1) following by expression of pSer9-GSK-3 β and generation of ROS.

Conclusions: The PI3K/Akt/GSK-3 β /ROS/eIF2B pathway could regulate NK cell activity and sensitivity of tumor cells to NK cells, which resulted in breast cancer growth and lung metastasis. Thus, GSK-3 β is a promising target of anti-tumor therapy.

KEYWORDS

GSK-3 β ; NK cells; NKG2D/NKG2DLs; ROS; eIF2B; breast cancer

Introduction

More than 522,000 people die from breast cancer every year, and it still remains the leading cause of cancer-related deaths in women¹. Glycogen synthase kinase-3 (GSK-3), a serine/threonine protein kinase, has two main subtypes: GSK-3 α and GSK-3 β , which have 98% similarity in the catalytic zone with slight difference at the N- and C-termini². While GSK-3 α is mainly involved in the process of glycogen

metabolism, the biological function of GSK-3 β is more complicated and more intensely correlated with cancer; it is over-expressed in various cancers, including breast cancer. The activity of GSK-3 β is regulated by phosphorylation/dephosphorylation at different sites; GSK-3 β can be inactivated when it is phosphorylated at Ser9 by diverse signaling pathways³. Akt, protein kinase A/C (PKA/PKC), p70 ribosomal S6 kinase (p70S6K), p90 ribosomal S6 kinase (p90Rsk)⁴⁻⁶, and protein phosphatases such as PP1 and PP2A can inactive GSK-3 β by phosphorylating it at Ser9⁷. Phosphorylation of GSK-3 β at Tyr216 by kinases, such as Fyn and proline-rich tyrosine kinase 2 (PYK2), and autophosphorylation can activate GSK-3 β ^{8,9}.

GSK-3 β has previously been considered a potential tumor suppressor due to its ability to be phosphorylated and to

*These authors contributed equally to this work.

Correspondence to: Chen Li and Yue Wang

E-mail: cli0616826@126.com and wangyue@nankai.edu.cn

Received August 13, 2018; accepted November 1, 2018.

Available at www.cancerbiomed.org

Copyright © 2019 by Cancer Biology & Medicine

target oncogenic molecules, including c-Jun, c-Myc, cyclin D1, and β -catenin¹⁰. Moreover, recent reports have also supported that GSK-3 β is a therapeutic target in cancer owing to its negative regulation of proliferation and survival of cancer cells¹¹⁻¹⁵. It has previously been reported that GSK-3 β is associated with breast cancer drug resistance after exposure to chemotherapeutic drugs, such as doxorubicin, anthracycline, and endocrine drug tamoxifen^{10,16}. Studies have shown that the activated GSK-3 β acted as a tumor suppressor by negatively regulating epithelial-mesenchymal transition and cancer cell cycle by regulation of Mcl-1, Snail degradation¹⁷⁻¹⁹. In addition, GSK-3 β inactivates EZH2, a histone methyltransferase, which plays an important role in tumorigenesis, and thus, suppresses breast cancer cell growth and migration²⁰. Despite pSer9-GSK-3 β being reported as a biomarker of poor clinical prognosis of breast cancer^{21,22}, the role of GSK-3 β in breast cancer remains controversial with its role in immunoregulation for breast cancer not well clarified.

Due to these abilities to spontaneously kill targeted cells without any prior sensitization or MHC restriction, natural killer (NK) cells play a significant role in infection, hematopoietic stem cell (HSC) transplantation, autoimmunity, as well as tumor immune surveillance²³. NK cells exhibit the cytotoxicity against a variety of “stressed” cells mainly by receptor-ligand specific recognition and binding²⁴, and a series of cytokines released by NK cells also function to kill target cells²⁵. The natural killer group 2 member D (NKG2D) is the most important activating receptor with multiple ligands (NKG2DLs). The MHC class I-related chain (MIC) A/B and the retinoic acid transcript-1/UL-16 binding proteins (RAET1/ULBP) 1-6, play a decisive role in anti-tumor immune surveillance²⁶. Similarly, murine NKG2D binds to retinoic acid early inducible 1 (Rae1) and H60 and ULBP-like transcript 1 (Mult-1)²⁷. NKG2D-NKG2DLs signals via the adaptor molecule DAP10 mediated by phosphoinositide 3-kinase (PI3K) and DAP10 and 12 in mice, and induces degranulation and/or cytokine production in cytotoxic effector cells²⁸.

Previous studies have reported that PI3K/Akt/mTOR and reactive oxygen species (ROS) induce M2 macrophage polarization²⁹, therefore, we studied the effect of PI3K/Akt/GSK-3 β and ROS on NK cells. ROS are produced in tumor cells mainly by NADPH oxidases of the NOX family³⁰ and mitochondrial respiratory chain complex (MRCC)^{31,32}, accompanied with a series of changes, including the opening of mitochondrial permeability transition pore³³. ROS signaling contributes to proliferation and survival of various tumors, and overproduction of ROS promotes cancer development mainly by inducing genomic

instability³⁴. Previous studies have shown that ROS could be a potential target of anticancer therapy^{35,36}. ROS could reduce the cytotoxicity of NK cells³⁷ and reverse the immune suppression. In addition, inhibiting ROS could upregulate the NKG2D/MICA³⁸. Eukaryotic initiation factor 2B (eIF2B), an important rate-limiting protein, catalyzes the guanine nucleotide exchange (GNE) reaction, dissociates GDP from eIF2 α -GDP, and releases GTP. The eukaryotic translational initiation factor 2 (eIF2), composed of α -, β -, and γ -subunits, plays a critical role during the first step of protein synthesis. In the presence of GTP, eIF2 interacts with initiator Met-tRNA, delivers it to 40S ribosomes, and forms the 43S pre-initiation complex³⁹. Once the conserved Ser51 of eIF2 α in the trimeric complex is phosphorylated, the nucleotide exchange activity of eIF2B is inhibited due to its enhanced interaction with eIF2 α ⁴⁰. Previous studies have demonstrated that activated GSK-3 β inhibits ROS⁴¹, and that ROS induces the phosphorylation of eIF2 α ⁴², which results in dysfunction of eIF2B, and consequently, alters the expression of target proteins. Therefore, the aim of our study was to explore the effect of this relationship on NK cells and to elucidate whether inactivated GSK-3 β downregulates the expression of NKG2DLs via ROS and eIF2B.

Materials and methods

Material and reagents

Cell culture materials were obtained from Corning (Shanghai, China). A ROS assay kit, Wortmannin, N-acetyl cysteine (NAC), and H₂O₂ were purchased from Beyotime Biotechnology (Shanghai, China). TWS119 was purchased from Selleck (Texas, U.S.A.). LY294002 was purchased from Promega (Madison, U.S.A.). Salubrinal was obtained from MCE China. CD107a (LAMP-1) ELISA kit were purchased from ElabScience (Wuhan, China), whereas, PGE2 and IFN- γ ELISA kits was purchased from Mlbio (Shanghai, China), and mouse RPS19 ELISA kits were purchased from SaiDongnan (Tianjin, China). Antibodies were purchased as follows: NKG2D and ULBP1 or Mult-1 (Proteintech, America), GSK-3 β (Boster, Wuhan, China), pSer9-GSK-3 β (Santa Cruz, CA, USA), Rae1 (Santa Cruz), H60 (R&D system, Minnesota, USA), pSer535-eIF2B (Eno Gene, Nanjing, China), and β -actin (Santa Cruz).

Mice

Female BALB/C mice (6 to 8 weeks old) were purchased from the Institute of Experimental Animals of the Chinese

Academy of Medical Sciences, and housed in a standard polypropylene cage containing sterile bedding under controlled temperature (23 ± 2 °C), humidity ($50\% \pm 5\%$), and light (10 h of light and 14 h of dark). All experimental procedures were approved by the medical ethics committee, Nankai University (No.NK23508677EA2018). Transplanted tumor mice model was established by subcutaneously injecting 1×10^6 4T1 cells near the second right mammary fat pad. Seven days later, 12 mice were divided randomly into different 3 groups (4 mice per group) and intraperitoneally injected with different drugs: Vehicle (100 μ L physiological saline), TWS119 (15 mg/kg), and LY294002 (5 mg/kg), all once a day for seven days. Tumor growth was measured by a caliper every three days and tumor volume was calculated according to the formula $V = (L * W^2) * 0.5$, where L and W refer to mid-axis length and width, respectively. The mice were sacrificed at the 28th day, eyeball blood was collected for ELISA, tumors were weighed by electronic balance, and partially stored at -70 °C, and the rest was fixed in formaldehyde solution. Lungs were stained with India ink to detect metastasis nodules according to the following protocol: isolate the trachea and inject 15% India ink into the lungs through the trachea until the lungs stop dilating, ligate the trachea to prevent the backflow of India ink, wash the lungs with Fekete's solution (70 mL 75% alcohol + 10 mL methanol + 5 mL glacial acetic acid + 15 mL distilled water), and analyze images to count the tumor nodules.

Cell culture

Murine breast cancer cell line, 4T1, and murine NK cell line, KY-1, were purchased from ATCC. Primary NK cells were obtained from fresh spleens of BALB/C mice. The mice spleen NK cell isolation optimizing system was purchased from Tianjin Haoyanguake Biological Product Co. Ltd. 4T1 cells were cultured in RPMI-1640 medium supplemented with 10% fetal bovine serum and 1% penicillin-streptomycin solution (100 \times) in a humidified atmosphere containing 5% CO₂ at 37 °C. Murine primary NK cells were isolated from fresh spleens by TBD Science Mouse NK Cell Separation Kit (TBD science, Tianjin, China). In brief, spleen was ground into single cell homogenate, and after adding separation reagents, NK cells were purified. Purified primary NK cells were cultured in RPMI-1640 medium supplemented with 10% fetal bovine serum, 1% penicillin-streptomycin solution (100 \times), 200 U/mL interleukin 2 (IL-2; PeproTech, Beijing, China) and 10 μ M β -mercaptoethanol in a humidified atmosphere containing 5% CO₂ at 37 °C. The drugs used in

the study were as below: TWS119 (0–10 μ mol/L, 24 h), LY294002 (30 μ mol/L, 12–16 h), H₂O₂ (250 μ mol/L, 24 h), and NAC (5 mmol/L, 24 h), and the supernatant of 4T1 cells was added to medium according to the ratio of 2:3 to culture NK cells.

ELISA assay

Eyeball blood was collected from mice, incubated at 37 °C for 30 min, then centrifuged at 3,000 rpm for 10 min, and the serum was transferred to a new micro-centrifuge tube. Supernatants were harvested after NK cells were incubated with 4T1 cells. Both the serum and the supernatants were prepared to analyze the concentration of related factors according to manufacturing instructions with mouse CD107a (LAMP-1), Prostaglandin E2 (PGE2), IFN- γ ELISA kits. The total protein from 4T1 cells was extracted and analyzed by the Mouse RPS19 ELISA kit. All the assays were performed in triplicates.

RT-PCR analysis and real time-PCR

Total RNA (1 μ g) was reversed transcribed into cDNA using EasyScript® First-Strand cDNA Synthesis SuperMix (TransGen Biotech, Beijing, China). RT-PCR was performed with a MyGene™ Series Peltier Thermal Cycler, PCR products were electrophoresed on 1.5% agarose gel and visualized by GelRed staining, and photographs were taken using a Gel Doc™ XR+ (BIO-RAD, USA). The real time-PCR reaction was carried out with TransScript top green real time-PCR supermix (TransGen, Beijing, China), and the Bio-Rad CFX Manager system (Bio-Rad, USA). The primers are described in **Table 1**.

Western blot analysis

4T1 cells or tumor tissue homogenate were solubilized in RIPA lysis buffer with 1% phosphatase inhibitors and 2% protease inhibitor on ice and cell lysates were isolated by centrifugation at 12,000 rpm for 20 min. Then, the supernatant was transferred to a new micro-centrifuge tube. Protein concentrations were determined using BCA protein assay kit (Beyotime, Shanghai, China), and the proteins were mixed with 5 \times loading buffer (protein: 5 \times loading buffer = 4:1) and boiled at 95 °C for 10 min. Proteins (30 μ g/lane) were loaded into the lanes of an SDS-polyacrylamide gel and separated by electrophoresis. The proteins were then transferred to PVDF membranes at 300 mA for 53 min. After

Table 1 Primer sequences

Genes	Forward primer	Reverse primer
GSK-3 β	CTTGGACAAAGGTCTCCGGCC	GTTGGCAGGCGGTGAAGCAG
H60	GCCTCAACAAATCGTCAT	ATACACCAAGCGAATACC
Rae1	GCT GTTGCC ACA GTC ACA TC	CCT GGGTACCT GAA GTC AT
NOX1	CCTGATTCTGTGTGTCGAAA	TTGGCTTCTCTGTAGCGTTC
NOX2	CCTCTACCAAAACCATTCCGGAG	CTGTCCACGTACAATTCGTTC
NOX3	CAAGTGTGTGCTGTAGAGGAC	CTATCCCGTAGGCAACGAGTT
NOX4	TTTCTCAGGTGTGCATGTAGC	GCGTAGGTAGAAGCTGTAACCA
eIF2b	AGTTCTAGTGCCGATAGCTT	AGCAGCAAAAGACAAATGTTTCC
CCND1	TGACTGCCGAGAAGTTGTGC	CTCATCCGCCTCTGGCATT
NFAT1	GGTTGCTCCTCTGCCCGCAG	TTGGAGGGGATCCCGCAGGG
NKG2D	ACGTTTCAGCCAGTATTGTGC	GGAAGCTTGCTCTGGTTC

blocking with 5% nonfat milk for at least 2 h, we incubated the membranes with anti-GSK-3 β , pSer9-GSK-3 β , H60, Rae1, pSer535-eIF2B, Mult-1, and β -actin antibodies overnight at 4 °C. After washing three times with 1 \times TBST, the membranes were incubated with secondary antibody for 1 h. Density analysis was performed using Image J2, and the experiments were repeated three times.

Flow cytometry

ROS level was examined with a ROS assay kit that sets DCFH-DA as the probe. Then we detected the intensity of the DCF signal by flow cytometry to quantify the intracellular production of ROS. 4T1 cells were trypsinized, incubated with DCFH-DA-containing serum-free medium for 20 min at 37 °C, centrifuged at 1,000 rpm for 5 min, discarded the supernatant, and then, washed three times with PBS. Cells were analyzed on BD FACS Canto II. Data were analyzed with FlowJo 7.6.

Cytotoxicity assay

4T1 cells treated with TWS119, LY294002, H₂O₂, and NAC were incubated with Calcein-AM. Then, the cells were incubated with freshly isolated NK cells for 4 h at various effector/target ratios. The fluorescence of each supernatant was measured at an excitation peak of 490 nm and an emission peak of 515 nm using the multispectral spectrophotometer. The percentage of specific lysis was calculated according to the following formula: the rate of specific lysis (%) = [(experimental release-spontaneous release)/(maximum release-spontaneous release)] \times 100%.

Transwell migration assay

The assay was performed in a 24-well Boyden chamber with 8- μ m pore size (Corning, Shanghai, China), and 4T1 cells (1×10^5) were seeded in the upper chamber with TWS119 for 24 h and LY294002 for 16 h, we fixed the undersurface cells of transwell chambers with methyl alcohol and stained them with 0.1% crystal violet. A Nikon Eclipse 80i microscope and Nikon Elements Imaging System Software were used to capture images of migrated 4T1 cells.

Immunohistochemistry (IHC)

Formalin-fixed and paraffin-embedded samples were cut into 5- μ m sections. Antigen retrieval was carried out by boiling in citrate buffer (pH 6.0), and the tissues were incubated with anti-GSK-3 β , anti-pSer9-GSK-3 β , anti-H60, anti-Rae1, and anti-pSer535-eIF2B antibody overnight, diaminobenzidine (DAB) was used for color development (Nikon Eclipse 80i). Visible nodules with weak or strong staining were counted under microscope. Mean densities in the plotted areas were quantitatively analyzed by the Image Pro Plus (IPP) software. More than ten views were used for the analysis each image, and three images of different treatment groups were selected randomly to perform analysis.

Mitochondrial ROS (mROS) measurement

mROS was measured using a MitoSOXTM Red mitochondrial superoxide indicator (YEASEN, Shanghai, China) according to the manufacturer's instructions. 4T1 cells were added in 24-well plate on the cover slip, after being treated with

TWS119, H₂O₂, and NAC for 24 h and LY294002 for 12 h. Cells of all groups were incubated with 5 μ M MitoSOXTM reagent working solution for 10 min at 37 °C in the dark. After washing three times with warm HBSS, we detected the ROS intensity with a fluorescent microscope.

Quantifying the activity of MRCC I/III

MRCC I/III kits (Solarbio, Beijing, China) were used according to manufacturer's instructions. 5×10^6 4T1 cells were collected to homogenate on ice, and the homogenate was then centrifuged at 600 rpm, 4 °C for 5 min, then we suspended the precipitant (mitochondria), and treated them by ultrasonication in ice bath (200 W, 3 s for 30 times, interval for 10 s). Forty microliters of samples were mixed with 800 μ L working solution, and recorded the initial absorbance (A1) and final absorbance after 2 minutes (A2) at 340 nm and 550 nm for MRCC I/III, respectively. The activity unit is defined as 1 nmol NADH or reduced CYC consumed by 10^4 cells per minute, and the activity was calculated as per the formulae: (1) activity of complex I (U/ 10^4 cells) = 0.73 (A1–A2), and (2) activity of complex III (nmol/min/ 10^4 cells) = 0.248 (A1–A2).

Statistical analysis

The data are presented as “mean \pm SE” and analyzed using SPSS 13.0. The differences between two groups were assessed by Student's *t*-test and the differences among three or more groups by one-way ANOVA followed by the Dunnett test. *P* < 0.05 is considered statistically significant.

Results

GSK-3 β inactivation promoted breast cancer growth and lung metastasis by suppressing the function of NK cells

To investigate the effects of GSK-3 β on breast cancer and cytotoxicity of NK cells, we performed a series of experiments in 4T1 cell-harboring mice treated with TWS119 (4,6-disubstituted pyrrolo-pyrimidine), which functions by phosphorylating GSK-3 β at Ser9. After the formation of subcutaneous transplanted tumors, BALB/C mice were intraperitoneally injected with TWS119 (15 mg/kg) once a day, continuously for seven days, while the control group mice were injected with normal saline at the same time points. The mice were sacrificed at the 28th day after the initial inoculation of 4T1 cells (Figure 1A). The tumors of

the treatment group were significantly larger than those of the control group, and the number of lung metastatic nodules, both in the front and back of the lung, also increased significantly compared to that in the control group (**P* < 0.05, Figure 1B). Then, to evaluate the cytotoxicity indirectly, we employed ELISA assay and the results showed that the levels of NK cell cytotoxic factors, CD107a and IFN- γ , decreased significantly in the TWS119 treatment group, and in contrast, the levels of inhibitory molecule PGE2 in NK cells increased (**P* < 0.05, Figure 1C). NK cells target the NKG2DLs of the tumor cells, and eliminate them. Therefore, we detected the expression of NKG2DLs by Western blot in fresh tumor tissue homogenate, and similarly, found that the levels of H60 and Rae1 in the TWS119 treatment group were attenuated compared with that in the control group (Figure 1D). Taken together, these data indicated that inactivated GSK-3 β could promote breast cancer growth and lung metastasis partly by suppressing the function of NK cells and the response of tumor cells to NK cells.

pSer9-GSK-3 β downregulated the expression of NKG2DLs and promoted the migration of 4T1 cells *in vitro*

TWS119 suppressed the function of NK cells, and promoted the growth and metastasis of breast cancer by phosphorylating GSK-3 β at Ser9. To further explore the role of GSK-3 β in breast cancer, we cultured 4T1 cells with different concentrations of TWS119. Our results revealed that the expression of NKG2DLs (H60 and Rae1) was downregulated after TWS119 treatment in concentration-dependent manner at both mRNA and protein levels; 2.5 μ mol/L TWS119 was selected as the optimum concentration based on the degree of GSK-3 β phosphorylation as detected by RT-PCR (Figure 2A), real time PCR (Figure 2B) and Western blot analysis (Figure 2C, **P* < 0.05, ***P* < 0.01). LY294002, a PI3K/Akt pathway inhibitor, exhibits the ability to decline the phosphorylation level as mentioned above, and was speculated to be an indirect activator of GSK-3 β . We found that 4T1 cells treated with 30 μ mol/L LY294002 significantly upregulated the expression of the NKG2DLs at both on mRNA and protein levels as observed with RT-PCR (Figure 2D), Real time PCR (Figure 2E), and Western blot analysis (Figure 2F, **P* < 0.05, ***P* < 0.01). The supernatant obtained from TWS119- and LY294002-treated 4T1 cells was used to culture primary NK cells (Figure 3A) and KY-1 cell line (Figure 3B), and results of RT-PCR and Western blot analysis showed that the expression of NKG2D was downregulated after inhibiting the GSK-3 β and was

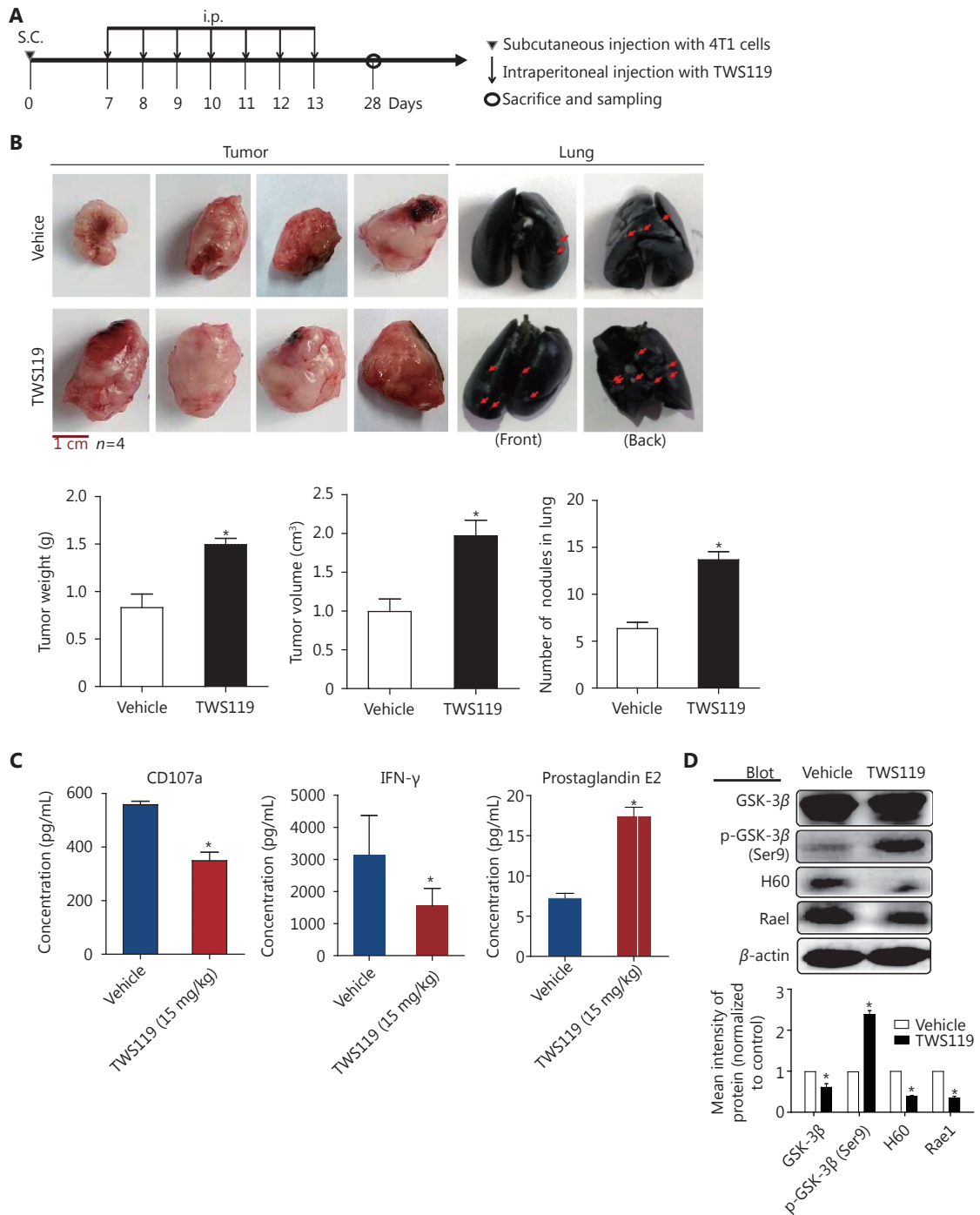


Figure 1 Inhibition of GSK-3 β promoted the tumor growth and suppressed NK function in 4T1 transplanted tumor mice. (A) Tumor transplantation method to establish mouse breast cancer animal model. (B) Representative images and quantification of tumor weight, tumor volume, and lung metastasis nodules in TWS119 (15 mg/kg)-treated tumor-bearing mice. (C) ELISA analysis of CD107a, IFN- γ , and PGE2 levels in eyeblood serum. *, indicates values with $P < 0.05$ vs. vehicle. (D) The expression of NKG2D ligands (H60 and Rae1) was analyzed by Western blot using tumor tissue homogenate.

upregulated after the GSK-3 β was indirectly activated. In addition, we performed a Calcein AM release assay to

determine the effects of GSK-3 β on the cytotoxicity of NK cells. Briefly, primary NK cells were obtained from spleen of

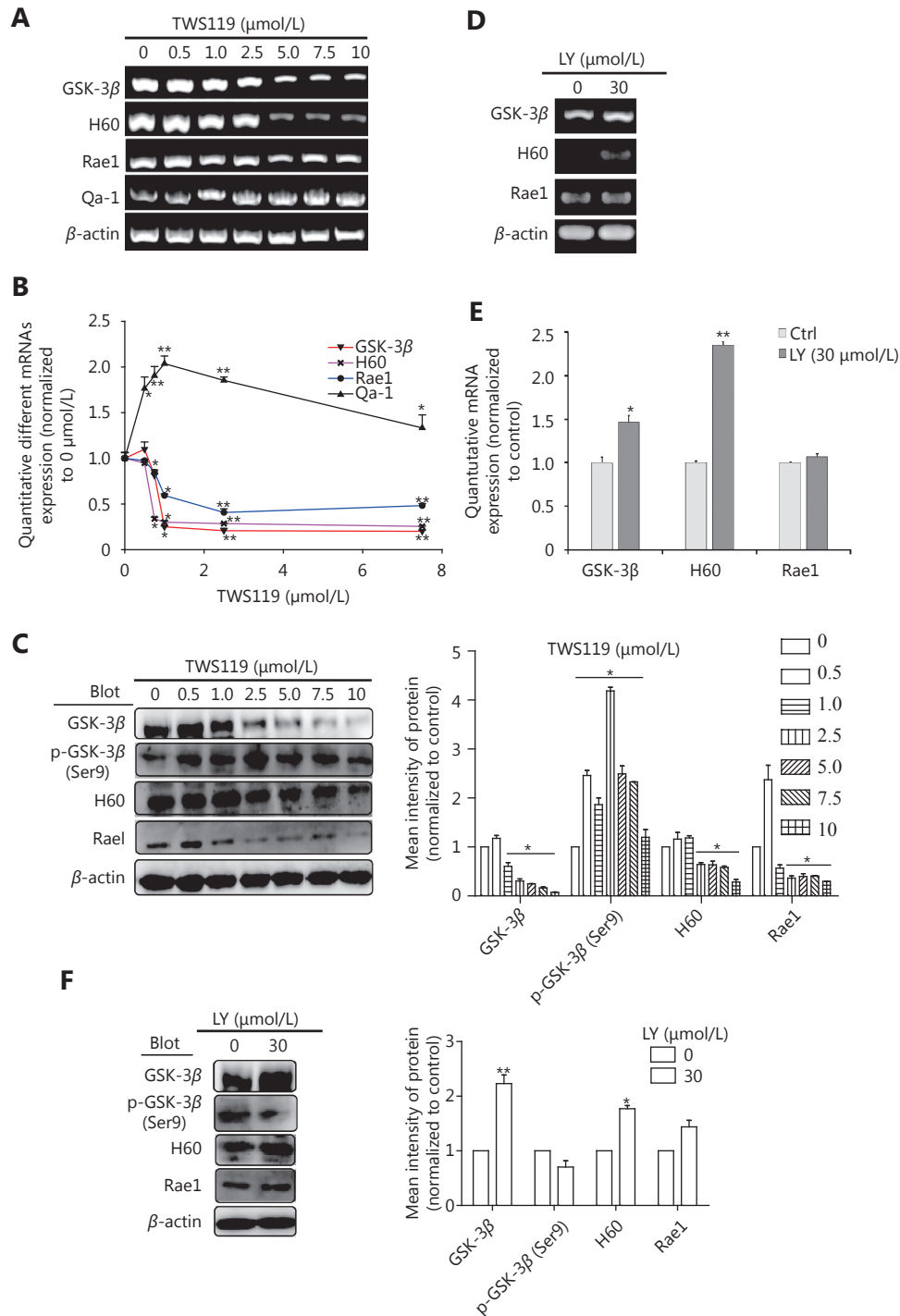


Figure 2 GSK-3 β upregulated the expression of NKG2D ligands. PCR (A) and Western blot (C) were performed in 4T1 cells to determine the expression of H60 and Rae1 or Qa-1 after treatment with inhibitor TWS119 (2.5 $\mu\text{mol/L}$). (B) Quantitative analysis of the PCR in 2A. PCR (D) and Western blot (F) were performed in 4T1 to determine the expression of H60 and Rae1 after treatment with GSK-3 β activator, LY294002 (30 $\mu\text{mol/L}$). (E) Quantitative analysis of the PCR in 2D. *, ** indicate values of $P < 0.05$, $P < 0.01$, respectively.

BALB/C mice by magnetic-activated cell-sorting, and then co-incubated with 4T1 cells at different effector/target ratios (E/T ratio). We observed that TWS119 lowered the activity of

NK cells, while LY294002 significantly promoted their activity ($*P < 0.05$, **Figure 3C**). Furthermore, transwell migration assay validated that pSer9-GSK-3 β contributed to

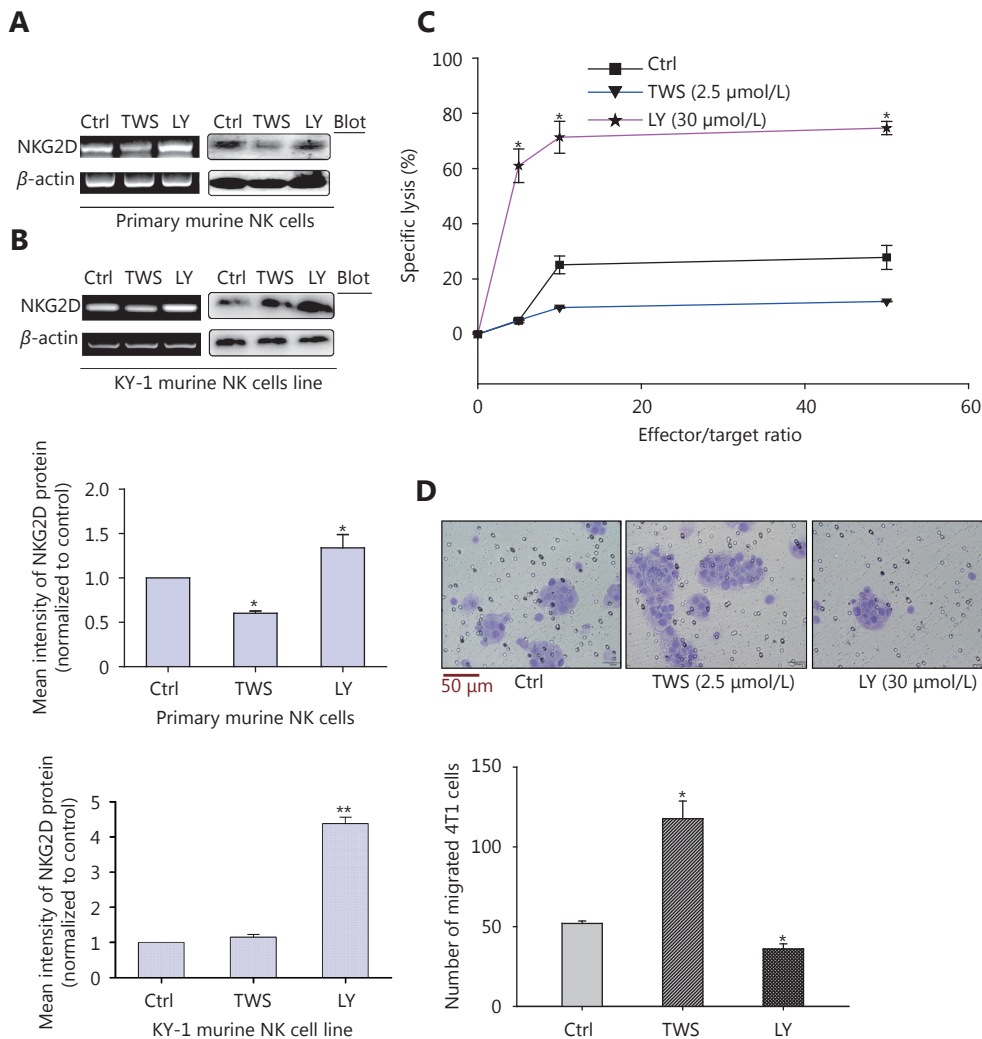


Figure 3 GSK-3β improved NK cell cytotoxicity and suppressed migration of 4T1 cells by upregulating the expression of NKG2D. After the treatment with TWS119 and LY294002, the expression of NKG2D in primary NK cells (A) and in mice NK cell line KY-1 (B) was assessed by RT-PCR and Western blot. (C) The cytotoxicity of NK cells was measured by Calcein AM-release assay. (D) The migration ability of 4T1 cells was detected by transwell migration assay. The migrated cells were quantified for 4 random fields. *, ** indicate values of $P < 0.05$, $P < 0.01$, respectively.

the migration of 4T1 cells *in vitro* ($*P < 0.05$, **Figure 3D**), which was consistent with the results of the lung metastases in animal experiments. Therefore, we concluded that the inhibition of PI3K/Akt/GSK-3β signaling promoted the cytotoxicity of NK cells and upregulated the expression of NKG2DLs on the surface of 4T1 cells, thereby suppressing the aggressiveness of tumor cells.

Intracellular ROS mediated the GSK-3β induced regulation of NK and 4T1 cells

Accumulating evidence has reported that GSK-3β function in

cancer via various classical signaling pathways, including Wnt/β-catenin, Ras/Raf/MEK/ERK, Notch, Hedgehog, and so on^{19,43}. It has also been shown that chronic ROS enhanced the growth and tumorigenic potential of the MCF7 breast cancer and it even activated various signaling pathways, such as PI3K/AKT³⁸. Therefore, we tried to further explore the correlation between ROS and GSK-3β. The data obtained from the flow cytometry analysis showed that the intracellular ROS change tendency was significantly different between TWS119 and LY294002-treated groups ($*P < 0.05$, **Figure 4A**). Compared with that in the control group, TWS119 inactivated GSK-3β and led to a higher ROS level.

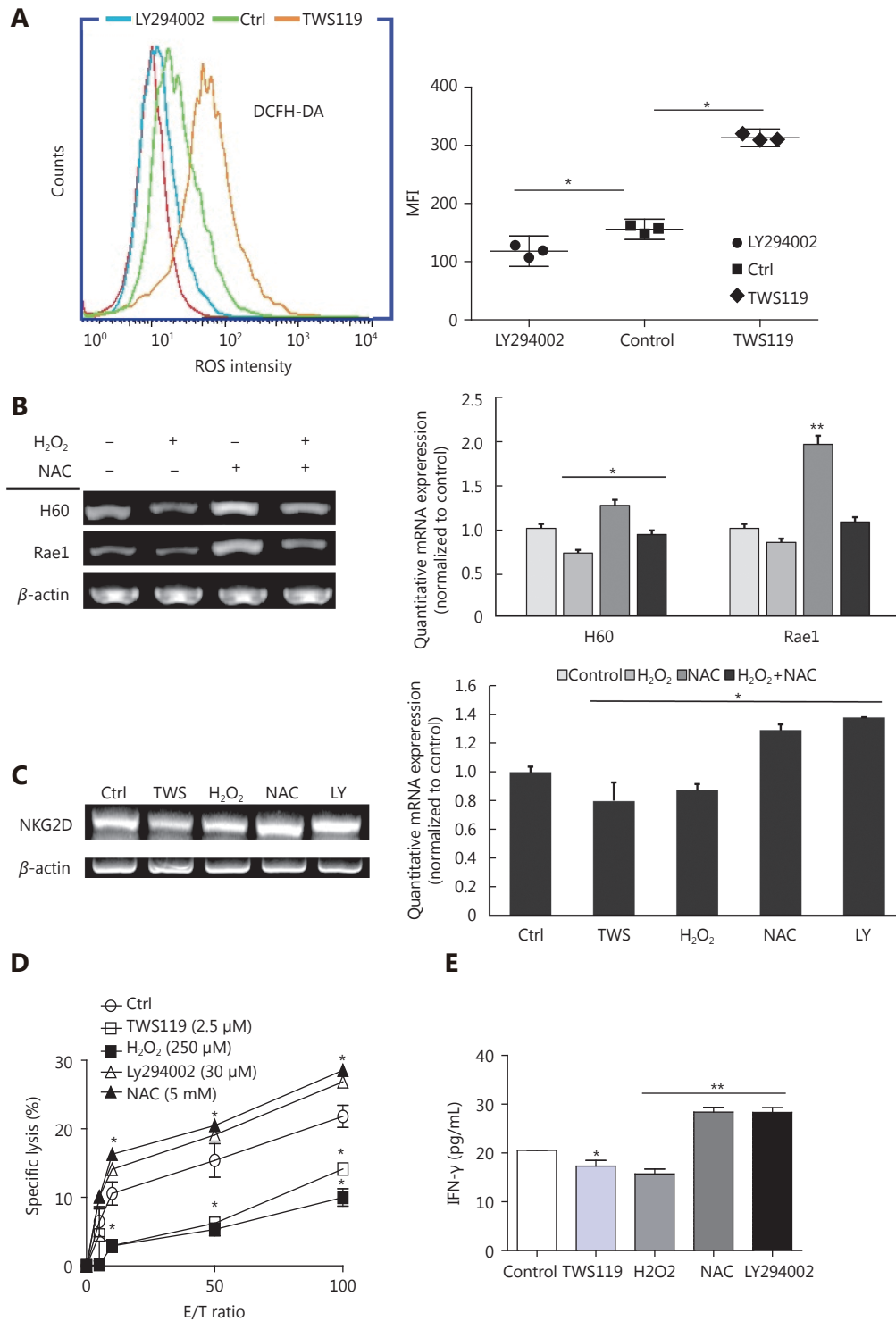


Figure 4 GSK-3 β enhanced NK cell function by attenuating the intracellular ROS production. (A) ROS levels of 4T1 cells, treated with TWS119 and LY294002, were determined by flow cytometry. (B) The expression of H60 and Rae1 was analyzed by RT-PCR and real time-PCR after H₂O₂ (250 μ mol/L) and NAC (5 mmol/L) treatment. (C, D, E) The expression of NKG2D, the cytotoxicity of NK cells, and IFN- γ concentration was evaluated by RT-PCR, real time-PCR, Calcein release assay, and ELISA. *, ** indicate values of $P < 0.05$, $P < 0.01$, respectively.

Does ROS affect the activity and the sensitivity of NK cells, at least partly? H_2O_2 (250 $\mu\text{mol/L}$) and N-acetylcysteine (NAC, a thiol antioxidant, 5 mmol/L) were used to induce and eliminate ROS, respectively, to answer this question. By RT-PCR and real time-PCR, we first detected the NK cell activation related ligands (H60 and Rae1) in different groups, and found that NAC could upregulate the expression of H60 and Rae1, which was contrary to the observation in the TWS119 group ($*P < 0.05$, $**P < 0.01$, **Figure 4B**). Then, the expression of NKG2D in primary NK cells was downregulated in TWS119- and H_2O_2 -treated groups, and was upregulated in LY294002- and NAC-treated groups ($*P < 0.05$, **Figure 4C**). Combined with the results from **Figure 3A**, we speculated ROS to be an important factor regulated by GSK-3 β , and ROS influenced the recognition and combination of NK cells to 4T1 cells via NKG2D-NKG2DLs. We also discovered that pSer9-GSK-3 β damaged the activity of NK cell via ROS. The results of Calcein release assay showed that TWS119 and H_2O_2 attenuated the direct cytotoxicity of NK cells while LY294002 and NAC enhanced their cytotoxicity (**Figure 4D**). Further, IFN- γ release, an indirect index of the NK cell cytotoxicity, exhibited the same trend ($*P < 0.05$, $**P < 0.01$, **Figure 4E**). To conclude, ROS was responsible for GSK-3-induced regulation of NK and 4T1 cells; therefore, activating GSK-3 β or inhibiting ROS could prove to be a potential anti-breast cancer therapy.

Mitochondrial ROS (mtROS) was mainly responsible for the regulation of NK cells by GSK-3 β

Commonly, mitochondria are the main sources of ROS. Therefore, we measured the potential changes in mitochondrial ROS. Firstly, we observed the distribution of mitochondrial ROS with a fluorescent dye, MitoSOX red, which specifically targets mitochondrial ROS. The results showed that TWS119 and H_2O_2 -treated groups significantly enhanced mtROS production, while NAC and LY294002 attenuated it. This change in mtROS level was in agreement with the change in intracellular ROS level, and the mtROS displayed a strong co-localization with mitochondria. Our results showed that ROS was indeed responsible for the dysfunction of mitochondria ($*P < 0.05$, **Figure 5A**).

Mitochondria produce ROS mainly via NOX and mitochondrial respiratory chain complex. In this study, using RT-PCR amplification and Western blot analysis, we initially found that NOX3 and NOX4 upregulated the expression by 1.5-fold and 2.3-fold on mRNA level, respectively. We also found NOX4 protein was upregulated after TWS119 and

downregulated after LY294002 treatment ($*P < 0.05$, **Figure 5B**), while NOX1 and NOX2 induced no such variation (data not shown). Besides, the activity of mitochondrial respiratory chain complex (MRCC) represents the electron flux during redox reaction, and partially reflects mitochondrial ROS status to some degree. By detecting the activity of MRCC, we indirectly evaluated the effect of GSK-3 β on ROS level, and this investigation proved that pSer9-GSK-3 β and H_2O_2 significantly upregulated the activity of MRCC I and III, whereas LY294002 and NAC downregulated the activity of MRCC I and III ($*P < 0.05$, **Figure 5C**).

pSer535-eIF2B was involved in the regulation of NK cells and tumor cells followed by GSK-3 β / ROS

GSK-3 β is a multifunctional molecule that regulates a variety of signaling pathways. Previous studies have revealed that CCND1 (cyclinD1), NFAT1 (nuclear factor of activated T cells), and eIF2B exhibited high expression levels in breast cancer cells and tissues, and the activated GSK-3 β phosphorylated these downstream molecules (CCND1, NFAT1, and eIF2B)⁴⁴⁻⁴⁶ to suppress the growth and metastasis of breast cancer.

Furthermore, we treated 4T1 cells with different concentrations of TWS119, performed RT-PCR and real time-PCR, and the results showed that eIF2B gradually decreased after the TWS119 treatment ($*P < 0.05$, $**P < 0.01$, **Figure 6A** and **6B**); however, the change in CCND1 and NFAT1 was obscure (data not shown). Study showed that ROS could inhibit the phosphorylation of eIF2B by oxidative modification of serine residue of ϵ subunit⁴⁷, which may partly explain how GSK-3 β affects eIF2B. We next found the expression of pSer535-eIF2B significantly decreased in TWS119-treated 4T1 cells, which was consistent with the tendency of the H_2O_2 group, whereas LY294002-, wortmannin-, NAC-, and SOD-treated groups exhibited opposite effects on the expression of pSer535-eIF2B (**Figure 6C**). These results further suggested that pSer535-eIF2B might be the downstream regulatory factor of GSK-3 β /ROS. Does pSer535-eIF2B affect the expression of NKG2DLs? We analyzed the tumor tissues obtained from animal experiments and found that, with the phosphorylation level of GSK-3 β decreased, the phosphorylation of eIF2B at Ser535 and the expression of H60 and Rae1 increased by Western blot analysis (**Figure 6D**) and IHC test ($*P < 0.05$, **Figure 6E**).

Therefore, we speculated that eIF2B might be one of the factors through which GSK-3 β regulated the expression of

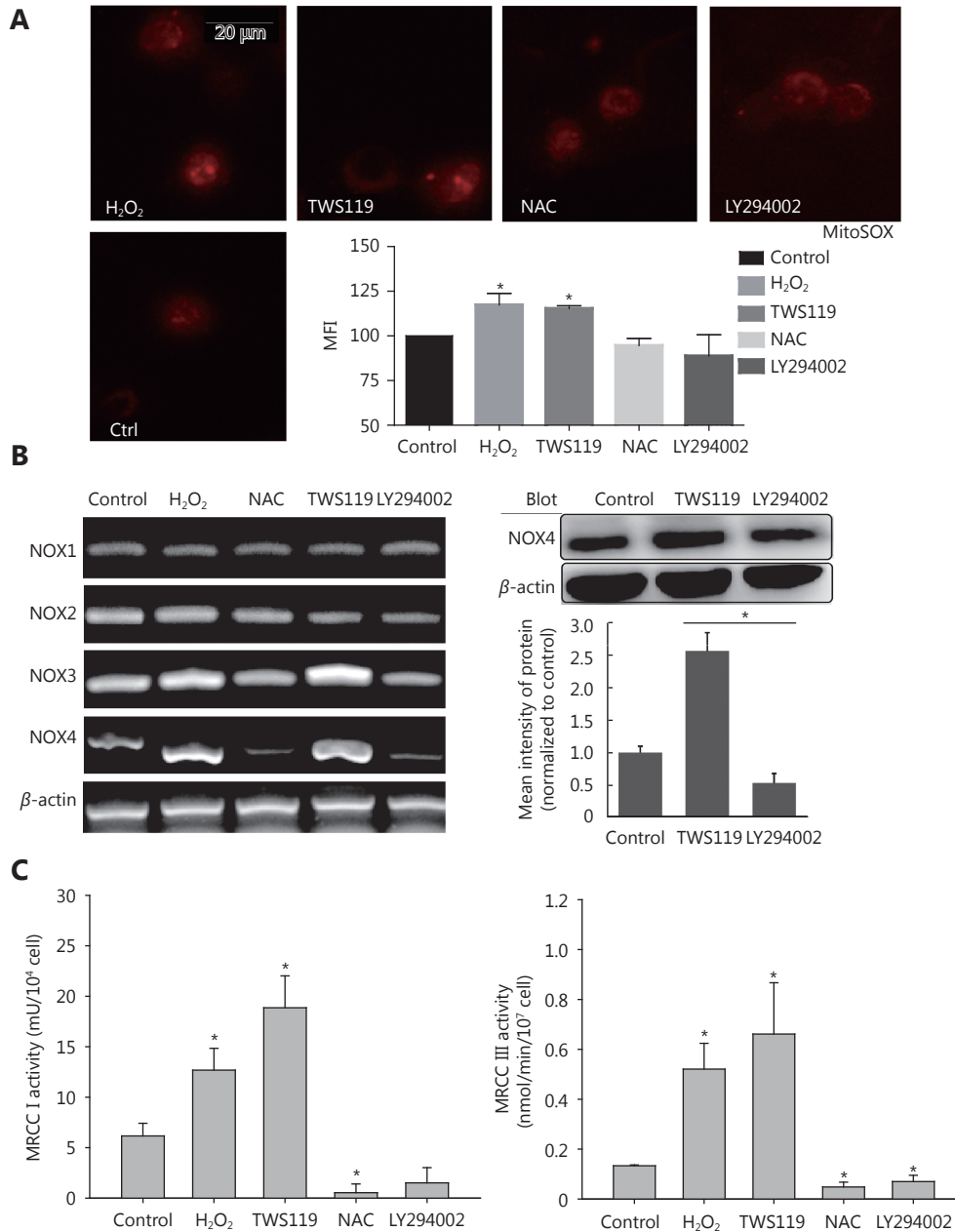


Figure 5 Attenuating mitochondrial ROS was mainly responsible for the improved function of NK cells after GSK-3 β treatment. (A) MitosoxTM fluorescence probe was used to observe mitochondrial ROS activity after treatment with TWS119, LY294002, H₂O₂, and NAC. (B) The expression of NOX1-4 was amplified by RT-PCR and NOX4 levels were further analyzed by Western blot. (C) The activity of MRCC I and III in 4T1 cells was determined by a multiscan spectrum microplate spectrophotometer. *, ** indicate values of $P < 0.05$ and $P < 0.01$, respectively.

NK cell ligands. To better understand the effect of eIF2B on NKG2DLs (Mult-1 and Rae1), we employed salubrinal, an eIF2 α dephosphorylation inhibitor, to combine and competitively inhibit the activity of eIF2B. Normally, eIF2 interacts with initiator Met-tRNA, forms the trimeric complex after recruitment by the RPS19 protein of the

ribosomal 40S subunit, and binds to ribosomal 60S subunit. After treatment with salubrinal, Ser51 of eIF2 α subunit is phosphorylated, eIF2B becomes inactivated, the ribosomal 60S subunit stops synthesizing, and finally, leads to the 40S reservoir.

To confirm the efficacy of salubrinal, we examined the

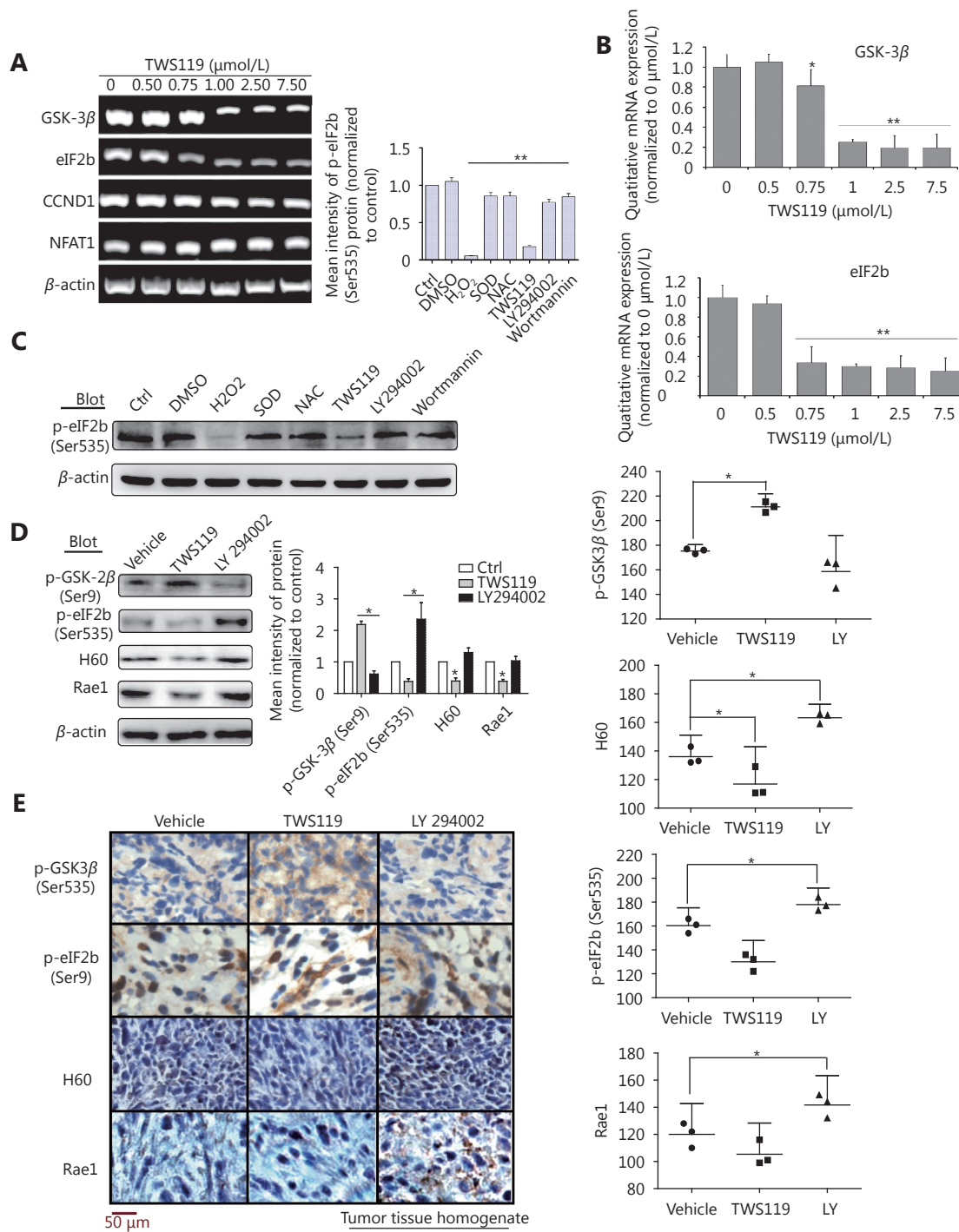


Figure 6 eIF2B functions as a downstream molecule of PI3K/AKT/GSK-3β/ROS pathway to upregulate NKG2D ligands. (A) eIF2B, CCND1, and NFAT1 levels were investigated by RT-PCR. (B) mRNA levels of GSK-3β and eIF2B, protein levels of pSer9-GSK-3β, pSer535-eIF2B, H60, and Rae1 were quantified. (C) The expression of p-eIF2B induced by H₂O₂, NAC, and SOD (1,000 U/mL) as well as TWS119, LY294002, and Wortmannin (2 μmol/L, another inhibitor of PI3K/AKT) was detected by Western blot. (D) The protein levels of p-GSK-3β, p-eIF2B, H60 and Rae1 expressed in tumor tissue homogenate after intraperitoneal injection of TWS119 and LY294002 (5 mg/kg) was assayed by Western blot. (E) Consecutive sections of above tissues were stained by DAB. The mean densities in the positive areas were quantitatively by the IPP software. *, indicates values of *P* < 0.05.

levels of ribosomal protein 40S by mouse RPS19 ELISA, and found the 40S retention was significantly enhanced after treatment with salubrinal (20 and 40 μ mol/L) (* P < 0.05, **Figure 7A**). The results of Western blot showed that the expression of Mult-1 and Rae1 was upregulated with increase in the phosphorylation of eIF2B after treatment with salubrinal in a concentration-dependent manner and 15 μ mol/L was optimal concentration (* P < 0.05, ** P < 0.01, **Figure 7B**). Given that eIF2B facilitates NK cells to kill tumor, in part because of robust expression of NKG2D and NKG2DLs, how does eIF2B affect the expression of NKG2D? Meta-analysis of 1023 breast cancer patients cataloged in StarBase v2.0 revealed a marked reduction in NKG2D mRNA levels with a decrease in expression of eIF2B1 and eIF2B3 (**Figure 7C**). We concluded that eIF2B influenced NKG2D despite the study number was relatively small (breast cancer patients: 998 samples vs. normal: 108 samples).

Finally, we can summarize that PI3K/Akt phosphorylated and inactivated GSK-3 β at Ser9, the inactivated GSK-3 β increased mitochondrial ROS, and subsequently, attenuated phosphorylation of eIF2B at Ser535, the rate-limiting factor of translation initiation, which might suppress the activity of NK cells by downregulating the expression of NKG2D and NKG2DLs (H60, Rae1, or Mult-1), and finally, promoted the growth and lung metastasis of mouse breast cancer (**Figure 7D**).

Discussion

GSK-3 β has been reported as both a tumor promoter as well as suppressor in different cancers, and is abnormally inactivated in breast cancer. In this study, the animal experiments demonstrated that inhibiting GSK-3 β by TWS119 promoted the growth and metastasis of mouse breast cancer, which was consistent with results of a previous study²⁰. The tumor progression is regulated by the immune cells in tumor microenvironment, and we found that inactivated GSK-3 β attenuated the activity of NK cell. In vitro studies also found that GSK-3 β regulated the cytotoxicity of NK cells and susceptibility of 4T1 cells to specific cytotoxicity.

Previous research has indicated that Akt activation led to the inactivation of GSK-3 β , which was related with poor clinical outcome²¹. As upstream molecules, both Akt and PKC can inhibit GSK-3 β by phosphorylating Ser9, and it has been reported that LY317615, a selective inhibitor of PKC, could effectively suppress the phosphorylation of GSK-3 β at Ser9⁴⁸. We used LY294002 to rescue the abnormal GSK-3 β . Results in our study showed that LY294002 slowed down the

migration and strengthened the susceptibility of 4T1 cells to specific cytotoxicity, while promoting the activity of NK cells. Despite NK cells being only a fraction of immune microenvironment, the discovery makes sense to modify NK cells and improve the response of tumor cells to NK cells. Given that chimeric antigen receptor (CAR)-NK cell- and NK cell activating receptors (NKR)-NK cell-based immunotherapies are promising new strategies for cancer therapy⁴⁹, and the promising results of this study lay foundation to accelerate the development and application of such immunotherapy.

A recent study showed that NOX2-derived ROS facilitated metastasis of melanoma cells by downregulating NK-cell function⁵⁰, and our study illuminated that TWS119 induced a higher-level of ROS by upregulating the expression of NOX3 and NOX4 in 4T1 cells. Therefore, we deduced and confirmed that such accumulated ROS further inhibited the function of NK cells and promoted lung metastasis in breast cancer mice model. At this point, our result was in line with that of a previous study, which indicated that NOX4 was a potential target for intervention of cancer metastasis⁵¹. Our results in this study may provide a novel strategy for intervening breast cancer by combined application of adoptive NK cells and NOX4 inhibitor or pharmaceutical inhibitor of GSK-3 β . However, the GSK-3 β pharmaceutical inhibitor always resulted in a serious drug resistance as a clinical reaction. Therefore, to enhance the anticancer potential⁵², we should focus on attenuating pSer9-GSK-3 β that may lead to drug resistance. Thus, NOX4 inhibitor is a better option, and must be studied further.

Besides, mitochondrial respiratory chain complexes are key sources of ROS generation and major regulators of cell apoptosis, among which complexes I and III are the most important⁵³. Our study indicated that the activity of complexes I and III was positively correlated with the phosphorylation of GSK-3 β at Ser9. Therefore, we can conclude mitochondrial respiratory chain complex is emerging as a novel target, and it could be regulated by pSer9-GSK-3 β in 4T1 cells. Previous studies have shown that the activity of complexes was most remarkable in most aggressive breast cancer and Mito-TAM, a novel mitochondrial-targeted derivative of tamoxifen, and suppressed HER-2 breast cancer via selective disruption of respiratory supercomplexes^{54,55}. Taking species differences and tumor heterogeneity into consideration, confirmation in human breast cancer tissue is still indispensable to get accurate conclusions.

In addition, we paid more attention to the phosphorylation of GSK-3 β at Ser9, which inactivates it,

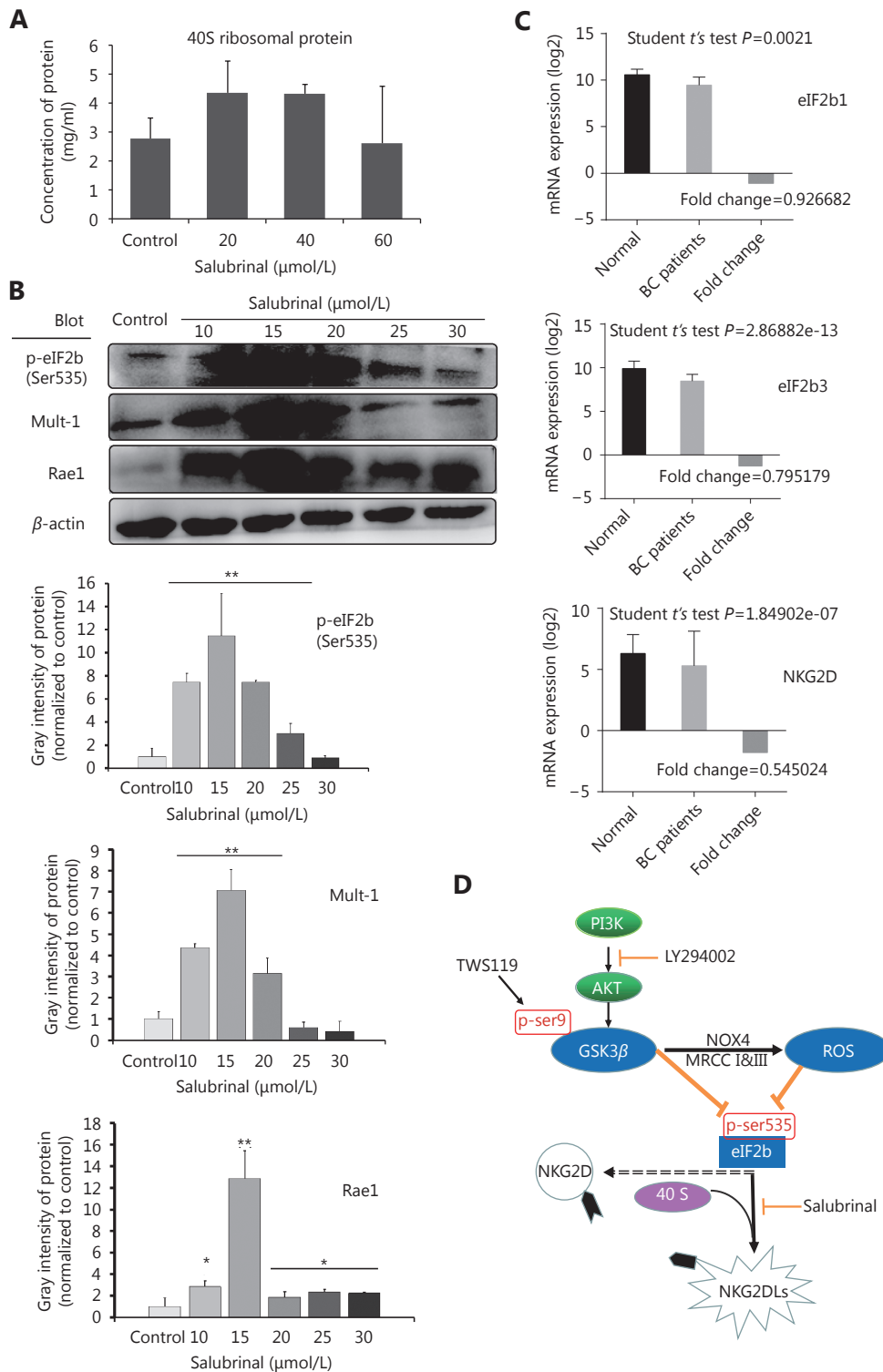


Figure 7 The cytotoxicity of NK cells was improved by inactivation of eIF2B. (A) The expression of RPS19 (a part of the ribosomal 40S subunit) was detected by ELISA to confirm the inhibition to eIF2B in the 4T1 cells after treatment with salubrinal. (B) The expression of NKG2D ligands (Rae1 and Mult-1) was upregulated after phosphorylation of eIF2B as detected by Western blot. (C) Meta-analysis showed that eIF2B1, eIF2B3, and NKG2D mRNAs expressed constitutively in human breast cancer patients (998 samples) and normal tissues (108 samples). (D) Schematic model of this study. *, ** indicate values of $P < 0.05$, $P < 0.01$, respectively.

while phosphorylation at Tyr216 site was not considered. Is there a balance in the regulation of the phosphorylation at Ser9 and Tyr216 sites? The problem has not been solved yet. Therefore, we have come to the conclusion that the inhibitor of GSK-3 β promoted the growth and metastasis of mouse breast cancer, but more experiments are needed to be performed to elucidate whether the direct activation of GSK-3 β can restore IFN γ -dependent, NK cell-mediated elimination of tumor cells.

Finally, eIF2B was identified to be regulated by ROS, which was induced by inactivated GSK-3 β . In fact, GSK-3 β regulates many downstream molecules by phosphorylating these substrates, some of which are tumor suppressors, such as phosphatase and tensin homolog deleted on chromosome ten (PTEN), and some of which are tumor promoters, such as C-myc. So GSK-3 β affects breast cancer via a comprehensive interaction of different signals, and as a downstream molecule of PI3K/Akt/GSK-3 β /ROS signaling pathway, among which eIF2B could be a major target. Since GSK-3 β inactivated eIF2B by phosphorylating eIF2B- ϵ Ser^{53,56}, and different studies have reported that ROS inactivated eIF2B by oxidative modification to the serine residue, overproduction of NAD⁺ and NADP⁺ caused by mitochondrial dysfunction could inhibit the activity of eIF2B⁵⁷, and results from our study showed that dysfunctional eIF2B upregulated NKG2DLs, we concluded that GSK-3 β /ROS/eIF2B plays an important role in regulation of the sensitivity of tumor cells to NK cells.

In summary, we demonstrated that GSK-3 β , a tumor suppressor, could regulate the activity of NK cells and the susceptibility of tumor cells by controlling the level of ROS, and therefore, could modulate cancer growth and metastasis. Combined with our previous study, which showed that ROS promotes isoprenaline-induced M2 macrophage polarization²⁹, the results in this study show ROS as a potential target for cancer therapy, and in particular, NOX4 treatment may be potentially used to disrupt breast cancer metastasis. It has been previously reported that $\gamma\delta$ T cells suppress cutaneous malignancy via NKG2D-associated regulation⁵⁸; therefore, it deserves further attention. In addition, it must be further studied if GSK-3 β /ROS plays a major role in T cell-mediated regulation of breast cancer, including $\gamma\delta$ T cells as well as integral T cell-related system.

The regulation of GSK-3 β /ROS/NOX4 axis must be further studied to develop novel therapeutic strategies for breast cancer. EGFR/RAS/RAF/MEK/ERK/MARP signaling is common in all kind of cancers, and double inhibition by BRAF (darafenib) and MERK (trametinib) have been approved for the treatment of NSCLC, melanoma, and

anaplastic thyroid cancer with BRAF V600E mutation by the FDA, based on the clinical trials for NCT01336634 and NCT02034110. Similarly, double inhibition by pSer9-GSK-3 β and NOX or eIF2B may prove to be a viable alternative option.

Acknowledgements

This work was supported by grants from the National Natural Science Foundation of China (Grant No. 8117975 and 31770968) and Tianjin Institutes for Basic Sciences (Grant No. 15JCYBJC26900 and 16JCQJNC11700). We thank Professor Phillip Bryant (Nankai University) and Chang Liu (Tianjin University of Sport, China) for linguistic support.

Conflict of interest statement

No potential conflicts of interest are disclosed.

References

1. Ferlay J, Soerjomataram I, Dikshit R, Eser S, Mathers C, Rebelo M, et al. Cancer incidence and mortality worldwide: Sources, methods and major patterns in globocan 2012. *Int J Cancer*. 2015; 136: E359-86.
2. Donovan GR, Baldo BA, Sutherland S. Molecular cloning and characterization of a major allergen (myr p i) from the venom of the australian jumper ant, *myrmecia pilosula*. *Biochim Biophys Acta*. 1993; 1171: 272-80.
3. McCubrey JA, Davis NM, Abrams SL, Montalto G, Cervello M, Basecke J, et al. Diverse roles of gsk-3: Tumor promoter-tumor suppressor, target in cancer therapy. *Adv Biol Regul*. 2014; 54: 176-96.
4. Sutherland C. What are the bona fide gsk3 substrates? *Int J Alzheimers Dis*. 2011; 2011: 505607.
5. Fang X, Yu SX, Lu Y, Bast RC, Jr., Woodgett JR, Mills GB. Phosphorylation and inactivation of glycogen synthase kinase 3 by protein kinase a. *Proc Natl Acad Sci U S A*. 2000; 97: 11960-5.
6. Tejada-Munoz N, Gonzalez-Aguilar H, Santoyo-Ramos P, Castaneda-Patlan MC, Robles-Flores M. Glycogen synthase kinase 3beta is positively regulated by protein kinase czeta-mediated phosphorylation induced by wnt agonists. *Mol Cell Biol*. 2015; 36: 731-41.
7. McCubrey JA, Steelman LS, Bertrand FE, Davis NM, Sokolosky M, Abrams SL, et al. Gsk-3 as potential target for therapeutic intervention in cancer. *Oncotarget*. 2014; 5: 2881-911.
8. Cole A, Frame S, Cohen P. Further evidence that the tyrosine phosphorylation of glycogen synthase kinase-3 (gsk3) in mammalian cells is an autophosphorylation event. *Biochem J*. 2004; 377: 249-55.

9. Medina M, Wandosell F. Deconstructing gsk-3: The fine regulation of its activity. *Int J Alzheimers Dis.* 2011; 2011: 479249.
10. Martelli AM, Buontempo F, Evangelisti C. Gsk-3beta: A key regulator of breast cancer drug resistance. *Cell Cycle.* 2014; 13: 697-8.
11. Shao J, Teng Y, Padia R, Hong S, Noh H, Xie X, et al. Cop1 and gsk3beta cooperate to promote c-jun degradation and inhibit breast cancer cell tumorigenesis. *Neoplasia.* 2013; 15: 1075-85.
12. Zhai L, Ma C, Li W, Yang S, Liu Z. Mir-143 suppresses epithelial-mesenchymal transition and inhibits tumor growth of breast cancer through down-regulation of erk5. *Mol Carcinog.* 2016; 55: 1990-2000.
13. Zeng J, Liu D, Qiu Z, Huang Y, Chen B, Wang L, et al. Gsk3beta overexpression indicates poor prognosis and its inhibition reduces cell proliferation and survival of non-small cell lung cancer cells. *PLoS One.* 2014; 9: e9123.
14. Zhang ZJ, Yang YK, Wu WZ. Bufalin attenuates the stage and metastatic potential of hepatocellular carcinoma in nude mice. *J Transl Med.* 2014; 12: 57.
15. Domoto T, Pyko IV, Furuta T, Miyashita K, Uehara M, Shimasaki T, et al. Glycogen synthase kinase-3beta is a pivotal mediator of cancer invasion and resistance to therapy. *Cancer Sci.* 2016; 107: 1363-72.
16. Sokolosky M, Chappell WH, Stadelman K, Abrams SL, Davis NM, Steelman LS, et al. Inhibition of gsk-3beta activity can result in drug and hormonal resistance and alter sensitivity to targeted therapy in mcf-7 breast cancer cells. *Cell Cycle.* 2014; 13: 820-33.
17. Zhang D, Fei F, Li S, Zhao Y, Yang Z, Qu J, et al. The role of beta-catenin in the initiation and metastasis of ta2 mice spontaneous breast cancer. *J Cancer.* 2017; 8: 2114-23.
18. McCubrey JA, Rakus D, Gizak A, Steelman LS, Abrams SL, Lertpiriyapong K, et al. Effects of mutations in wnt/beta-catenin, hedgehog, notch and pi3k pathways on gsk-3 activity-diverse effects on cell growth, metabolism and cancer. *Biochim Biophys Acta.* 2016; 1863: 2942-76.
19. Aristizabal-Pachon AF, Castillo WO. Role of gsk3beta in breast cancer susceptibility. *Cancer Biomark.* 2017; 18: 169-75.
20. Ko HW, Lee HH, Huo L, Xia W, Yang CC, Hsu JL, et al. Gsk3beta inactivation promotes the oncogenic functions of ezh2 and enhances methylation of h3k27 in human breast cancers. *Oncotarget.* 2016; 7: 57131-44.
21. Armanious H, Deschenes J, Gelebart P, Ghosh S, Mackey J, Lai R. Clinical and biological significance of gsk-3beta inactivation in breast cancer-an immunohistochemical study. *Hum Pathol.* 2010; 41: 1657-63.
22. Quintayo MA, Munro AF, Thomas J, Kunkler IH, Jack W, Kerr GR, et al. Gsk3beta and cyclin d1 expression predicts outcome in early breast cancer patients. *Breast Cancer Res Treat.* 2012; 136: 161-8.
23. Narni-Mancinelli E, Vivier E, Kerdlies YM. The 't-cell-ness' of nk cells: Unexpected similarities between nk cells and t cells. *Int Immunol.* 2011; 23: 427-31.
24. Brumbaugh KM, Binstadt BA, Leibson PJ. Signal transduction during nk cell activation: Balancing opposing forces. *Curr Top Microbiol Immunol.* 1998; 230: 103-22.
25. Fauriat C, Long EO, Ljunggren HG, Bryceson YT. Regulation of human nk-cell cytokine and chemokine production by target cell recognition. *Blood.* 2010; 115: 2167-76.
26. Mincheva-Nilsson L, Baranov V. Cancer exosomes and nkg2d receptor-ligand interactions: Impairing nkg2d-mediated cytotoxicity and anti-tumour immune surveillance. *Semin Cancer Biol.* 2014; 28: 24-30.
27. Diefenbach A, Jensen ER, Jamieson AM, Raulet DH. Rae1 and h60 ligands of the nkg2d receptor stimulate tumour immunity. *Nature.* 2001; 413: 165-71.
28. Chang YH, Connolly J, Shimasaki N, Mimura K, Kono K, Campana D. A chimeric receptor with nkg2d specificity enhances natural killer cell activation and killing of tumor cells. *Cancer Res.* 2013; 73: 1777-86.
29. Shan M, Qin J, Jin F, Han X, Guan H, Li X, et al. Autophagy suppresses isoprenaline-induced m2 macrophage polarization via the ros/erk and mtor signaling pathway. *Free Radic Biol Med.* 2017; 110: 432-43.
30. Brandes RP, Weissmann N, Schroder K. Nox family nadph oxidases: Molecular mechanisms of activation. *Free Radic Biol Med.* 2014; 76: 208-26.
31. Sena LA, Chandel NS. Physiological roles of mitochondrial reactive oxygen species. *Mol Cell.* 2012; 48: 158-67.
32. Selivanov VA, Votyakova TV, Pivtoraiko VN, Zeak J, Sukhomlin T, Trucco M, et al. Reactive oxygen species production by forward and reverse electron fluxes in the mitochondrial respiratory chain. *PLoS Comput Biol.* 2011; 7: e1001115.
33. Zorov DB, Juhaszova M, Sollott SJ. Mitochondrial reactive oxygen species (ros) and ros-induced ros release. *Physiol Rev.* 2014; 94: 909-50.
34. Sabharwal SS, Schumacker PT. Mitochondrial ros in cancer: Initiators, amplifiers or an achilles' heel? *Nat Rev Cancer.* 2014; 14: 709-21.
35. Ralph SJ, Rodriguez-Enriquez S, Neuzil J, Saavedra E, Moreno-Sanchez R. The causes of cancer revisited: "Mitochondrial malignancy" And ros-induced oncogenic transformation - why mitochondria are targets for cancer therapy. *Mol Aspects Med.* 2010; 31: 145-70.
36. Yang Y, Karakhanova S, Hartwig W, D'Haese JG, Philippov PP, Werner J, et al. Mitochondria and mitochondrial ros in cancer: Novel targets for anticancer therapy. *J Cell Physiol.* 2016; 231: 2570-81.
37. Mimura K, Kua LF, Shimasaki N, Shiraiishi K, Nakajima S, Siang LK, et al. Upregulation of thioredoxin-1 in activated human nk cells confers increased tolerance to oxidative stress. *Cancer Immunol Immunother.* 2017; 66: 605-13.
38. Ke M, Wang H, Zhou Y, Li J, Liu Y, Zhang M, et al. Sep enhanced the antitumor activity of 5-fluorouracil by up-regulating nkg2d/mica and reversed immune suppression via inhibiting ros and caspase-3 in mice. *Oncotarget.* 2016; 7: 49509-26.
39. Rajesh K, Iyer A, Suragani RN, Ramaiah KV. Intersubunit and interprotein interactions of alpha- and beta-subunits of human

- eif2: Effect of phosphorylation. *Biochem Biophys Res Commun.* 2008; 374: 336-40.
40. Sudhakar A, Ramachandran A, Ghosh S, Hasnain SE, Kaufman RJ, Ramaiah KV. Phosphorylation of serine 51 in initiation factor 2 alpha (eif2 alpha) promotes complex formation between eif2 alpha(p) and eif2b and causes inhibition in the guanine nucleotide exchange activity of eif2b. *Biochemistry.* 2000; 39: 12929-38.
 41. Cheng Y, Xia Z, Han Y, Rong J. Plant natural product formononetin protects rat cardiomyocyte h9c2 cells against oxygen glucose deprivation and reoxygenation via inhibiting ros formation and promoting gsk-3beta phosphorylation. *Oxid Med Cell Longev.* 2016; 2016: 2060874.
 42. Rajesh K, Krishnamoorthy J, Kazimierczak U, Tenkerian C, Papadakis AI, Wang S, et al. Phosphorylation of the translation initiation factor eif2alpha at serine 51 determines the cell fate decisions of akt in response to oxidative stress. *Cell Death Dis.* 2015; 6: e1591.
 43. Verma NK, Fazil MH, Ong ST, Chalasani ML, Low JH, Kottaiswamy A, et al. Lfa-1/ICAM-1 ligation in human T cells promotes Th1 polarization through a GSK3beta signaling-dependent Notch pathway. *J Immunol.* 2016; 197: 108-18.
 44. Eo HJ, Park GH, Jeong JB. The involvement of cyclin D1 degradation through GSK3beta-mediated threonine-286 phosphorylation-dependent nuclear export in anti-cancer activity of mulberry root bark extracts. *Phytomedicine.* 2016; 23: 105-13.
 45. Yoeli-Lerner M, Chin YR, Hansen CK, Toker A. Akt/protein kinase B and glycogen synthase kinase-3beta signaling pathway regulates cell migration through the NFAT1 transcription factor. *Mol Cancer Res.* 2009; 7: 425-32.
 46. Weiss CS, Ochs MM, Hagenmueller M, Streit MR, Malekar P, Riffel JH, et al. Dyrk2 negatively regulates cardiomyocyte growth by mediating repressor function of GSK-3beta on eIF2Bepsilon. *PLoS One.* 2013; 8: e70848.
 47. Hohn A, Konig J, Grune T. Protein oxidation in aging and the removal of oxidized proteins. *J Proteomics.* 2013; 92: 132-59.
 48. Graff JR, McNulty AM, Hanna KR, Konicek BW, Lynch RL, Bailey SN, et al. The protein kinase C beta-selective inhibitor, enzastaurin (LY317615.HCl), suppresses signaling through the Akt pathway, induces apoptosis, and suppresses growth of human colon cancer and glioblastoma xenografts. *Cancer Res.* 2005; 65: 7462-9.
 49. Hu Y, Tian ZG, Zhang C. Chimeric antigen receptor (CAR)-transduced natural killer cells in tumor immunotherapy. *Acta Pharmacol Sin.* 2018; 39: 167-76.
 50. Aydin E, Johansson J, Nazir FH, Hellstrand K, Martner A. Role of NOX2-derived reactive oxygen species in NK cell-mediated control of murine melanoma metastasis. *Cancer Immunol Res.* 2017; 5: 804-11.
 51. Zhang B, Liu Z, Hu X. Inhibiting cancer metastasis via targeting NADPH oxidase 4. *Biochem Pharmacol.* 2013; 86: 253-66.
 52. Ugolkov A, Gaisina I, Zhang JS, Billadeau DD, White K, Kozikowski A, et al. GSK-3 inhibition overcomes chemoresistance in human breast cancer. *Cancer Lett.* 2016; 380: 384-92.
 53. Acin-Perez R, Fernandez-Silva P, Peleato ML, Perez-Martos A, Enriquez JA. Respiratory active mitochondrial supercomplexes. *Mol Cell.* 2008; 32: 529-39.
 54. Koit A, Shevchuk I, Ounpuu L, Klepinin A, Chekulayev V, Timohhina N, et al. Mitochondrial respiration in human colorectal and breast cancer clinical material is regulated differently. *Oxid Med Cell Longev.* 2017; 2017: 1372640.
 55. Rohlenova K, Sachaphibulkij K, Stursa J, Bezawork-Geleta A, Blecha J, Endaya B, et al. Selective disruption of respiratory supercomplexes as a new strategy to suppress HER2(high) breast cancer. *Antioxid Redox Signal.* 2017; 26: 84-103.
 56. Wang X, Paulin FE, Campbell LE, Gomez E, O'Brien K, Morrice N, et al. Eukaryotic initiation factor 2b: Identification of multiple phosphorylation sites in the epsilon-subunit and their functions in vivo. *EMBO J.* 2001; 20: 4349-59.
 57. Dholakia JN, Mueser TC, Woodley CL, Parkhurst LJ, Wahba AJ. The association of NADPH with the guanine nucleotide exchange factor from rabbit reticulocytes: A role of pyridine dinucleotides in eukaryotic polypeptide chain initiation. *Proc Natl Acad Sci U S A.* 1986; 83: 6746-50.
 58. Girardi M, Oppenheim DE, Steele CR, Lewis JM, Glusac E, Filler R, et al. Regulation of cutaneous malignancy by gamma delta T cells. *Science.* 2001; 294: 605-9.
- Cite this article as:** Jin F, Wu Z, Hu X, Zhang J, Gao Z, Han X, et al. The PI3K/Akt/GSK-3 β /ROS/eIF2B pathway promotes breast cancer growth and metastasis via suppression of NK cell cytotoxicity and tumor cell susceptibility. *Cancer Biol Med.* 2019; 16: 38-54. doi: 10.20892/j.issn.2095-3941.2018.0253